STAFF SUMMARY SHEET

	TO	ACTION	SIGNATURE (Surname), GRADE AND DATE		TO	ACTION	SIGNATURE (Surname), GRADE AND DATE
1	DFAN	sig	[signature] Lt Col, USAF 18 MAY 15	6			
2	DFER	approve	SOLIS, HD 25, 18 May 15	7			
3	DFAN	action	(Author /Originator)	8			
4				9			
5				10			

SURNAME OF ACTION OFFICER AND GRADE	SYMBOL	PHONE	TYPIST'S INITIALS	SUSPENSE DATE
Dr Chuck Wisniewski	DFAN	333-5182	CFW	20150601

SUBJECT	DATE
Clearance for Material for Public Release USAFA-DF-PA-	20150518

SUMMARY

1. PURPOSE. To provide security and policy review on the document at Tab 1 prior to release to the public.

2. BACKGROUND.
Authors: Charles F. Wisniewski, Aaron R. Byerley, William H. Heiser, Kenneth W. Van Treuren and William R. Liller

Title: The Influence of Airfoil Shape, Tip Geometry, Reynolds Number and Chord Length on Small Propeller Performance and Noise

Circle one: Abstract Tech Report Journal Article Speech Paper Presentation Poster
Thesis/Dissertation Book Other: _____

Check all that apply (For Communications Purposes):
[] CRADA (Cooperative Research and Development Agreement) exists
[] Photo/ Video Opportunities [] STEM-outreach Related [] New Invention/ Discovery/ Patent

Description: An extensive experimental investigation to determine the overall efficiency and near field noise signature of propellers utilized by small hand launched UASs has been conducted. This investigation has included wind tunnel performance comparisons of both off-the-shelf and custom designed propellers at realistic thrust and freestream velocities. A propeller design program has been developed that gives a user the ability to quickly design a propeller, predict its performance, and then create a 3D model in SolidWorks for fabrication using an SLA printer.

Release Information: To be presented at the 33rd AIAA Applied Aerodynamics Conference
22 - 26 June 2015 | Dallas, Texas

Previous Clearance information: (If applicable): SOCOM was the sponsor of this research and has endorsed public release.

Recommended Distribution Statement: Distribution A: approved for public release, distribution unlimited

3. DISCUSSION.

4. RECOMMENDATION. Sign coord block above indicating document is suitable for public release. Suitability is based solely on the document being unclassified, not jeopardizing DoD interests, and accurately portraying official policy.

Thomas E. McLaughlin, Ph.D.
Director, Aeronautics Research Center

The Influence of Airfoil Shape, Tip Geometry, Reynolds Number and Chord Length on Small Propeller Performance and Noise

Charles F. Wisniewski,* Aaron R. Byerley.† and William H. Heiser‡
USAF Academy, CO, 80132

Kenneth W. Van Treuren§ and William R. Liller, III**
Baylor University, Waco, TX, 76798

An extensive experimental investigation to determine the overall efficiency and near field noise signature of propellers utilized by small hand launched UASs has been conducted. This investigation has included wind tunnel performance comparisons of both off-the-shelf and custom designed propellers at realistic thrust and freestream velocities. A propeller design program has been developed that gives a user the ability to quickly design a propeller, predict its performance, and then create a 3D model in SolidWorks for fabrication using an SLA printer. This computer code was used to design propellers for a parametric study of airfoil cross-section, chord length and tip geometry which led to an optimized design configuration that greatly out performs available off-the-shelf propellers. The results of this design approach are high pitch propellers with low aspect ratios. The increased chord lengths create large surface areas that lower the rotational speed required to achieve the desired thrust for a given freestream velocity flight condition. These low aspect ratio propeller designs place emphasis on tip geometry to increase aerodynamic efficiency and reduce noise generating vortex strength. The result is a 5 bladed oval tipped propeller configuration that is *12 dB* quieter than the stock commercial propeller and *6% percent* more aerodynamically efficient. *This represents an elimination of 70% of the baseline propeller near-field noise signature with the potential of increasing the aircraft endurance by 6%.*

Nomenclature

A	=	through flow area (perpendicular to the station local velocity), in^2
A_p	=	propeller area, in^2
c_d	=	blade section drag coefficient
c_l	=	blade section lift coefficient
C_D	=	blade total drag coefficient
C_L	=	blade total lift coefficient
C_P	=	power coefficient
C_T	=	thrust coefficient
D	=	propeller blade drag, lb_f
D	=	propeller outer diameter, in
J	=	advance ratio
L	=	propeller blade lift, lb_f
$\dot{m}$	=	mass flow rate, lb_m/s
p	=	static pressure, lb_f/ft^2
P	=	power, W
P_h	=	pitch of blade, in
r	=	arbitrary radius, in
RPM	=	rotational speed, *revolutions per minute*
R	=	propeller outer radius, in

* Propulsion Research Associate, Department of Aeronautics, USAF Academy, and Senior Member.
† Professor, Department of Aeronautics, USAF Academy, and Associate Fellow.
‡ Professor Emeritus, Department of Aeronautics, USAF Academy, and Honorary Fellow.
§ Professor, Department of Mechanical Engineering, Baylor University #97356, and Senior Member.
** Graduate Student, Department of Mechanical Engineering, Baylor University #97356, and Student Member.

SPL = sound pressure level, *dB*
T = propeller thrust, lb_f
UAS = unmanned aerial system
V = velocity, *ft/s*
V_{rw} = relative wind velocity, ft/s
V_t = tangential propeller velocity, ft/s

Greek
α = angle of attack or blade incidence angle of flow, *deg*
β = angle of blade relative to circumferential or tangential, *deg*
ΔKE = change in kinetic energy, $ft\ lb_f$
γ = local flow angle relative to circumferential or tangential, *deg*
η_{aero} = propeller aerodynamic efficiency
η_o = propeller overall mechanical efficiency
η_{th} = propeller thermodynamic efficiency
η_p = propeller propulsive efficiency
ρ = density of air, lb_m/ft^3
τ = torque on propeller, $ft\text{-}lb_f$
ω = propeller rotational speed, *rad/s*

Subscripts
1, 2, 3, 4 = axial stations
0.75 = arbitrary ACC radial location of propeller blade quantities

I. Introduction

THE importance of the Unmanned Aerial System (UAS) is increasing as more tasks are being assigned to these vehicles. The term UAS highlights the systems nature of the vehicle to include the unmanned aircraft, propulsions system, control system and communications or telemetry link. Each is designed to support a particular mission. Since a majority of these vehicles are used for intelligence, surveillance, and reconnaissance (ISR), sensors are an important part of the system. Regardless of the mission and propulsion system, the customer always desires additional sensor capability and/or to remain on station for the longest possible period of time. This results in a tradeoff as the UAS has a limited amount of internal power from which to draw for its mission. If the propulsion system is more efficient, less power would be required for flight allowing for a longer endurance time. Thus, the guiding principle for this research effort is to examine an existing propulsion system for a current UAS and to seek ways to improve both the propulsive efficiency and decrease noise. This paper will examine high pitch propellers with low aspect ratios which result in increased chord lengths, as seen in Fig. 1. These large surface areas lower the rotational speed required to achieve the desired thrust for a given freestream velocity flight condition. The importance of the proper selection for the tip geometry is thought to increase aerodynamic

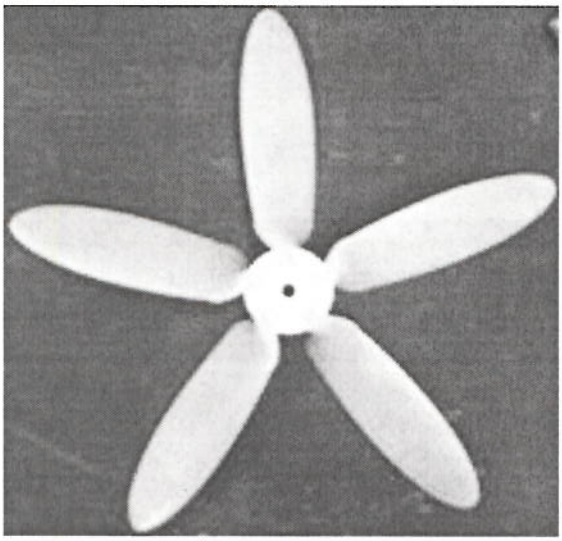

Figure 1. Five bladed oval tipped propeller configuration.

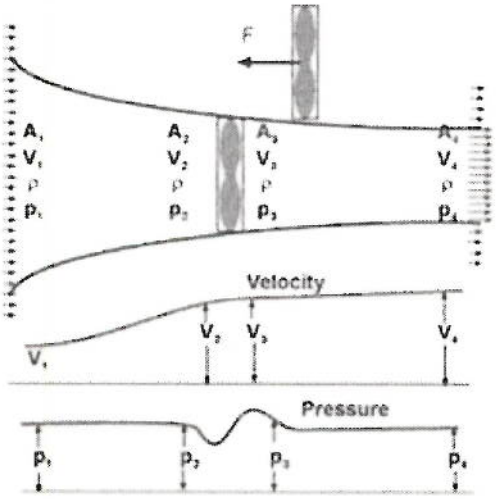

Figure 2. Open propeller depiction of inlet areas as well as changes in velocity and pressure in spatial relation to the propeller inlets.[1]

efficiency and reduce noise generating vortex strength.

A. Analysis

An open propeller propulsive system adds mechanical work to the flow of air around the propeller increasing the air velocity to produce thrust. The propeller has an airfoil cross-section that varies in twist and chord length in the radial direction. As the motor spins the propeller draws air in from an area, A_1, to the face of the propeller with area, A_2. The propeller adds mechanical work to the flow which directly increases the static pressure of the flow stream. Continuity for the incompressible flow being considered here requires that the area immediately downstream of the propeller, A_3, be the same as the upstream area A_2. This is depicted in Fig. 2. The higher static pressure then expands back to atmospheric pressure increasing the velocity and reducing the flowstream area to A_4. The propellers interaction with the flow and the size of areas result in the thrust used to propel the UAS.

The performance of the open propeller is characterized by the coefficient of thrust, C_T, coefficient of power, C_P, and overall efficiency, η_o.

$$C_T = \frac{T}{\rho N^2 D^4} \tag{1}$$

$$C_p = \frac{P}{\rho N^3 D^5} \tag{2}$$

$$\eta_o = J\frac{C_T}{C_p} = \frac{V_1 T}{P} \tag{3}$$

The coefficient of thrust is a dimensionless measure of thrust produced by the propeller where T is thrust, ρ is density, N is propeller rotational speed, and D is the diameter of the propeller. Thrust is simply the mass flow rate of air multiplied by the increase in air velocity created by the propeller

$$T = \dot{m}(V_4 - V_1) \tag{4}$$

For the UAS motor, power is based on the amount of torque produced by the propeller and the motor speed.

$$P = \tau N \tag{5}$$

The propulsive efficiency is the amount of thrust produced for a given power input. For an aircraft with a specified thrust required, a higher efficiency will result in better aircraft endurance. To achieve this, the exit velocity of the open propeller must be very close to the free stream velocity. The coefficient of thrust, coefficient of power, and the propulsive efficiency are functions of the advance ratio, J, which is given by

$$J = \frac{V_1}{ND} \tag{6}$$

The advance ratio is the distance the tip of the propeller will travel (advance) in one revolution for a given flight speed and is related to the angle of attack (AoA) the flow sees as the propeller rotates and moves through air.

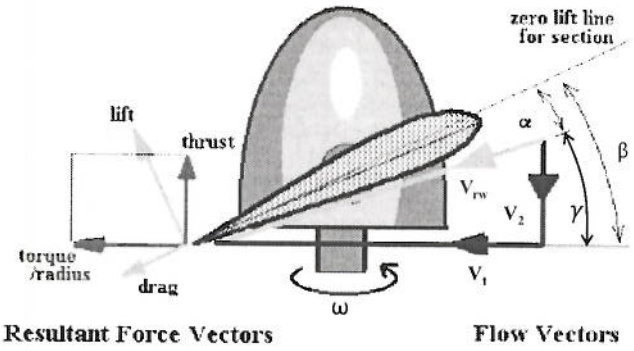

Figure 3. Velocity and force vectors on a rotating propeller blade.[2]

The chord length, airfoil shape of the blade, relative angle of attack, and Reynolds number all further describe and characterize the propeller and dictate its performance. In simple terms a propeller works as an airfoil spinning about the hub generating lift that provides forward thrust for the aircraft. A propeller has a relative angle of attack based on its radius, pitch, free stream velocity, and rotational speed (RPM). Figure 3 shows the cross-section of a propeller that is rotating into the page. The relative wind velocity (V_{rw}) at any given propeller cross-section is the vector sum of the incoming propeller blade velocity (V_2) and the tangential velocity ($V_t = \omega r$) for that cross-section which form the inflow angle γ. The angle of attack that the propeller experiences at a given cross-section is then the difference between the inflow angle and the local geometric twist of the propeller (β):

$$\alpha = \beta - \gamma \tag{7}$$

The blade pitch, P_b, is defined at the 0.75 radial location as (see Fig. 3)

$$P_b = 0.75(2\pi R)tan\beta_{r/R=0.75} \tag{8}$$

where R is the propeller outer radius and β is the angle between the angular flow velocity and the zero lift line of the airfoil section.

$$V_2 = \frac{V_1+V_4}{2} \tag{9}$$

$$T = \dot{m}(V_4 - V_1) = \rho A_P V_2 (V_4 - V_1) = \frac{\rho A_P}{2}(V_4^2 - V_1^2) \tag{10}$$

$$V_4 = \sqrt{\frac{2T}{\rho A_P} + V_1^2} \tag{11}$$

$$\tan(\gamma) = \frac{V_2}{\omega r} \tag{12}$$

$$\alpha = \beta - tan^{-1}\left(\frac{V_2}{\omega r}\right) \tag{13}$$

It is standard practice to maintain a constant angle of attack across the span of the propeller in an attempt for the propeller to operate near the maximum lift to drag ratio. The radial dependence of V_2 causes the inflow angle (γ) to change in the radial direction requiring the β angle to change in the radial direction in order to keep the angle of attack (α) the same for specified rotational and freestream velocities. This results in the familiar twist of a propeller with large β angles near the hub and lower angles near the tip. Each cross-section of the propeller generates lift and drag based on the aerodynamic characteristics of the airfoil section. The lift and drag forces can be resolved into forces in the thrust and torque directions which dictate the performance of the propeller at the specified operating conditions.

The overall efficiency of an engine is typically defined by the product of propulsive and thermal efficiency. Since the electrically driven system being studied here does not undergo a thermodynamic cycle, the thermal efficiency can be replaced with the aerodynamic efficiency of the propeller itself.

$$\eta_o = \eta_P \eta_{aero} = \frac{TV_1}{\tau N} \tag{14}$$

where TV_1 is the amount of mechanical power put into the propeller and τN is the amount of thrusting power available to the aircraft for propulsion. This represents the overall mechanical efficiency and does not take into account the electrical conversion efficiency of the motor and circuitry that supplies the motor. The propulsive efficiency represents how well the system utilizes the rate of kinetic energy generated by the propeller into thrusting power to the aircraft. It can be shown that the propulsive efficiency is only a function of the streamtube exit velocity (V_4) and the freestream velocity (V_1).[3]

$$\eta_P = \frac{TV_1}{\Delta \dot{K}E} = \frac{2}{1 + \frac{V_4}{V_1}} \tag{15}$$

The propulsive efficiency goes up as the exit velocity (V_4) decreases and reaches a maximum of 1.0 when $V_4 = V_1$. For a given thrust requirement, propulsive efficiency increases with increasing propeller diameter due to the decreasing V_4. The aerodynamic efficiency represents how well the propeller converts the mechanical power (τN) from the motor shaft into the rate of kinetic energy of the air. It can be shown that the aerodynamic efficiency is a function of the three dimensional lift to drag ratio of the propeller and the inflow angle.[3]

$$\eta_{aero} = \eta_{th} = \frac{\Delta \dot{K}E}{\tau N} = \frac{1 - \frac{C_D}{C_L} tan\gamma}{1 + \frac{C_D}{C_L} \frac{1}{tan\gamma}} \tag{16}$$

Increasing the aerodynamic efficiency requires increasing the three dimensional lift to drag ratio of propeller blade. This can be accomplished by designing the blade twist distribution so that each radial cross-section is at the angle of attack for maximum L/D, selecting an airfoil cross-section with high lift to drag, and designing a propeller tip to reduce induced drag.

B. Aero-Acoustic Modeling

In recent times reducing the detectability or noise of UAS vehicles has become important. Much of the noise or sound pressure level (SPL) of the UAS is generated by the blades of the propeller. The noise or SPL generated by a propeller is almost impossible to model correctly. This is because (1) there are many complex sources of noise, many of which depend on Reynolds number and minor details of the blade geometry, (2) the noise or SPL generated by a propeller blade depends on radial location along the propeller blade, and (3) the noise or SPL field is a function of frequency band, direction, and distance (in other words, the noise or SPL detected by observers depends on their hearing and location, and it changes as the UAS passes by).

II. Propeller Experimental Testing

A. Testing Background

A topic of increasing importance in the UAS community is the design and performance of open propellers used in hand launched, small UASs. The performance of these small propellers directly influences the operational capabilities of the UAS. As such, the design and testing of these propellers is necessary to accurately predict UAS performance. A previous experimental investigation examined the relationship between diameter, pitch, and number of blades to aerodynamic efficiency and aero-acoustic SPLs.[4] Thrust, torque, propeller rotational speed, and sound pressure level were measured for twelve aero-nautCAMcarbon (ACC) folding propeller configurations currently being used on an operational UAS with diameters ranging from 12 to 15 inches, pitches from 6 to 13 inches, and increasing from two to three propeller blades. Each configuration was tested at 44 ft/s tunnel velocity, the typical cruising velocity of a small UAS, while the propeller rotational speed was varied to determine the rotational speed needed to produce 2.5 lb_f of thrust, a typical cruise thrust required for a small UAS. As expected, the rotational speed required to achieve the desired thrust decreased approximately 7.7% per inch of increase in the propeller diameter. At the same time, the noise signature decreased by approximately 0.8 dB per inch increase and overall

efficiency rose by 2.9% per inch increase. Similar results were found for increasing both the number of propeller blades and also increasing the pitch of the propeller. Increasing from two to three blades decreased the rotational speed by 9.1% with a 2.1 dB drop in sound pressure level and an increase in overall efficiency of 3.2%. Increasing the pitch generally decreased rotational speed by 4.6% per inch of pitch increase and decreased noise level by 0.7 dB per inch of pitch increase. Overall efficiency slightly increased by 0.6% for an inch increase in pitch. For a given diameter propeller there seems to be an optimum pitch for minimum sound level. For design, this indicates there is an optimum angle of attack for the propeller, which translates to an optimum beta twist angle, to achieve minimum sound level. Noise generation was found to be a strong function of propeller rotational speed. Lower rotational speed produces less noise.

B. Experimental Propeller Testing Facility

The North Low-Speed Wind Tunnel (LSWT) at the USAF Academy was used to test all propellers in this test series (see Fig. 4). This tunnel is an Engineering Design Laboratory, Inc. tunnel with a test section of 36" x 36" x 40" that has a top speed of approximately 33 m/s. Due to the size of the test section and the diameter of the propellers tested, no wind tunnel corrections were incorporated into the data analysis. The motor being tested is from an operational UAS and was adapted to the thrust stand with a custom mount. The motor had an operating range of 15 to 26 VDC and up to 65 A. Tests for this series of experiments was accomplished with the power supply set to 24 VDC which allowed the motor to consume the current appropriate for the throttle setting. Power consumed by the motor was supplied by an HP 6269B DC Power supply (0 to 40 V, 0 to 50 A). The voltage was measured directly and the current was measured with a POWERTEK CTH/50/10/SC/24 VDC which has a range of 0 to 50 ADC. Measurements for the power were made immediately after the power supply and before the motor controller. Control for the motor was accomplished using a standard FUTABA R/C model system which drove a Phoenix ICE2 motor controller. The thrust is measured using a Transducer Techniques LSP-2 capable of a 0 to 2 kg (0 to 4.4 lb_f) measurement. Propeller torque is measured with an Interface MRT-2NM torque transducer capable of measuring 0 to 2 NM (0 to 17.7 inch-lb_f). . The thrust and torque load cells were calibrated by hanging known weights in line with each of the load cells. To measure the RPM, an OMEGA Remote Optical Sensor, model HHT-20 ROS, was used. Tunnel velocity is measured using a pitot-static tube, located upstream of the test section, and a Baratron MKS 220DD differential pressure transducer with a 0 to 10 torr (0 to 5.35 inches of water) range. All data were recorded using an Agilent 1421B VXI mainframe with an EC 1431C 64-Channel Scanning A/D card as well as anEC1415A Closed Loop Controller card.

An important part of these experiments were the measurement of SPLs for each of the propellers tested. The microphone used for these tests was a Brüel & Kjær 2230 Sound Level Meter capable of measuring 20 to 140 dB with an accuracy of +/- 2 dB. The directional sound level meter was located on the floor of the wind tunnel approximately 5 inches below and 2 inches aft of the tip of the propeller. In this configuration the microphone measures the near field noise signature of the propeller and simulates the conditions that would be experienced as the UAS flies overhead.

The uncertainties of all of the calculated results described in the above equations were determined using the root-sum-square uncertainty method from Kline and McClintock.[5] The uncertainty in overall efficiency was determined to be 1.4% with the largest part coming from the precision error of the velocity measurement. The sound pressure

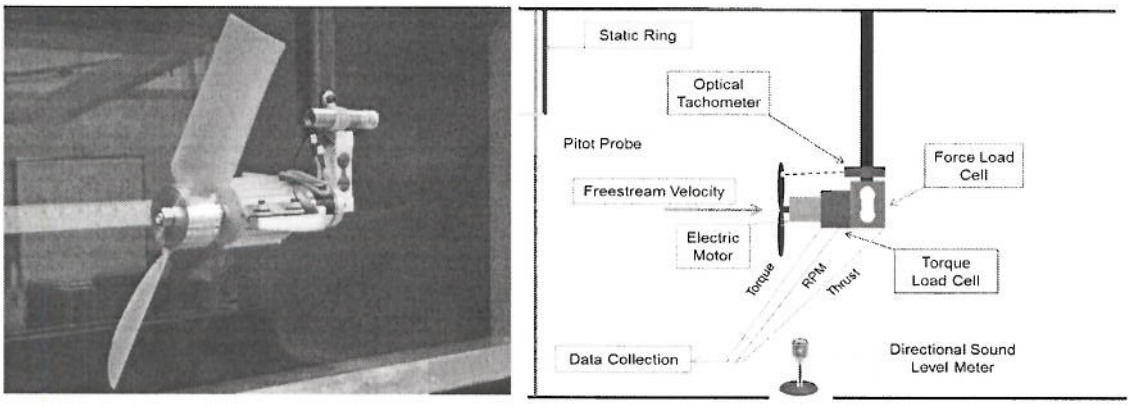

Figure 4. Custom propeller and motor mounted on test rig.[4]

Table 1. Lift and drag coefficient at AoA for maximum lift to drag ratio. Data taken from UIUC low Reynolds number database.[6]

Airfoil	AoA	Cl	Cd	Cl/Cd
ClarkY	7.6	1.0	0.0211	48.1
GM15	5.1	1.0	0.0130	76.9
Geo417	7.1	1.1	0.0164	65.5
FX63-137	9.3	1.5	0.0342	44.4

level uncertainty was estimated to be 0.61 dB or 0.71% which was nearly entirely attributed to the 0.55 dB accuracy of the microphone sound level calibrator (General Radio type 1562A). In practice the repeatability of the SPL measurements was ~0.2 dB.

Two independent propeller investigations were conducted. The first looked at the effect of propeller airfoil cross-section and the other into the effect of propeller tip geometry. During each investigation a series of propellers were designed, fabricated, and tested at the same operating conditions. The results of these two projects were then combined in an investigation of a set of hybrid propellers that combined the best airfoil and the best tip treatment and then extended to include multi-bladed propellers. The result is a propeller configuration seen in Fig. 1 that is 12 dB quieter than the baseline commercial ACC 13x10 propeller and 6 percentage points more efficient.

C. Airfoil Propeller Experimental Results

Most small propeller manufacturers use the Clark Y airfoil as it has a relatively flat bottom to the airfoil which makes it easy to manufacture and is structurally sound. From an aerodynamic viewpoint however, the Clark Y is not necessarily the best airfoil particularly at low Reynolds numbers (< 200,000). Other airfoils also have similar performance but, because of a lower drag value, might have a higher L/D_{max} value. Of these airfoils, the Clark Y, GM15, GOE 417 and FX63-137 were chosen from the University of Illinois, Urbana-Champaign (UIUC) database to compare as a full propeller design because of their low Reynolds number characteristics.[6] Figures 5 a,b show C_l and C_l/C_d vs AoA for these airfoils, respectively. Table 1 lists the maximum C_l/C_d and the AoA that it occurs for the four airfoils. Three propellers were designed for each airfoil cross-section with beta angle twist distributions to maintain a constant angle of attack over the span of the propeller at the specified operating condition. The AoA for each airfoil/propeller combination design were set at -2, 0 and +2 degrees from the AoA for maximum C_l/C_d for the airfoil. This gave a set of 12 propellers (three for each airfoil) with different lift and drag characteristics for testing and comparison, as shown in Table 2. The propellers were designed using the QMIL and QPROP propeller design and analysis programs developed by Drela[7] and incorporated in a Matlab GUI propeller design program called BEARCONTROL.[8] The design condition for all the propellers was to produce $2.5lb_f$ of thrust at 4,000 RPM and all had an overall diameter of 13.3 in.

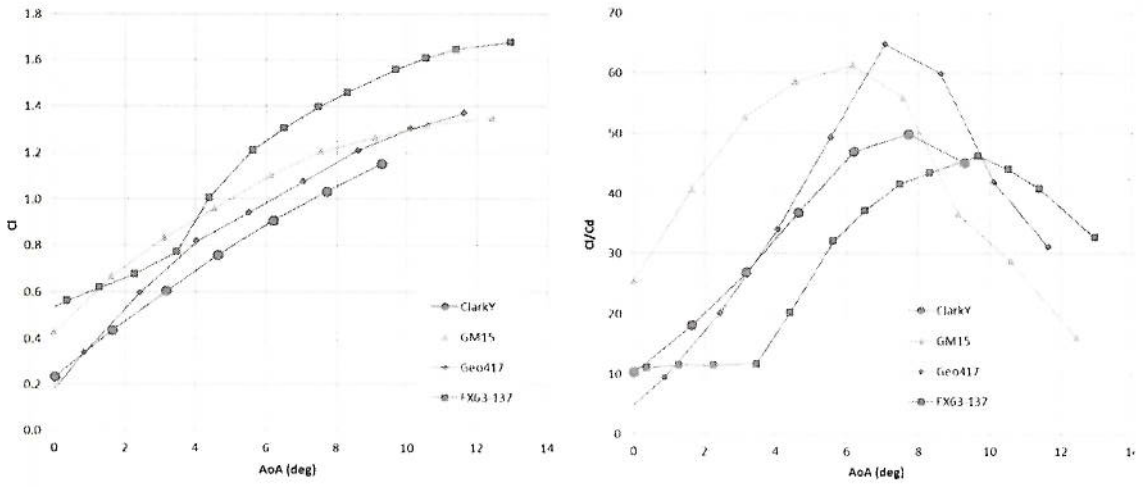

Figure 5 a, b. C_l vs AoA and C_l/C_d vs AoA curves respectively for airfoils initially examined.[6]

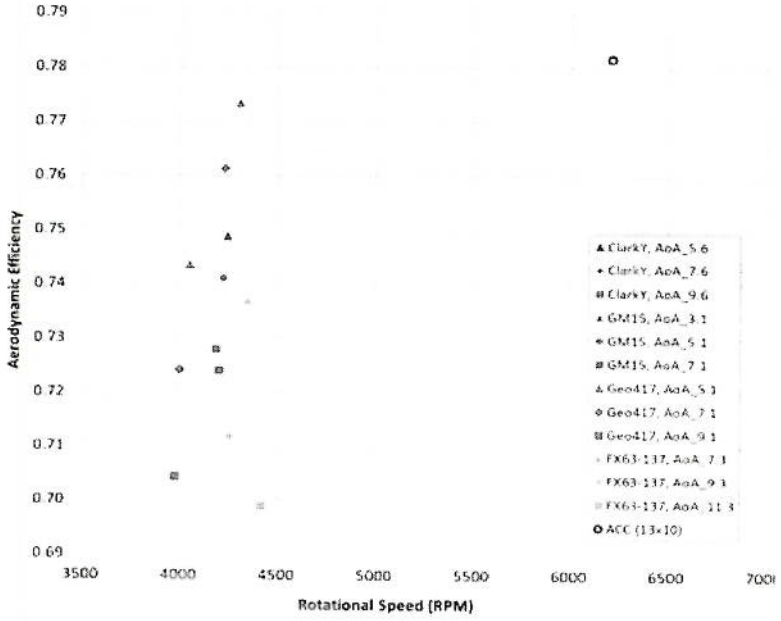

Figure 6. Aerodynamic efficiency as a function of the rotational speed required to achieve 2.5lb$_f$ of thrust at a freestream velocity of 44ft/s for the 12 airfoil propellers.

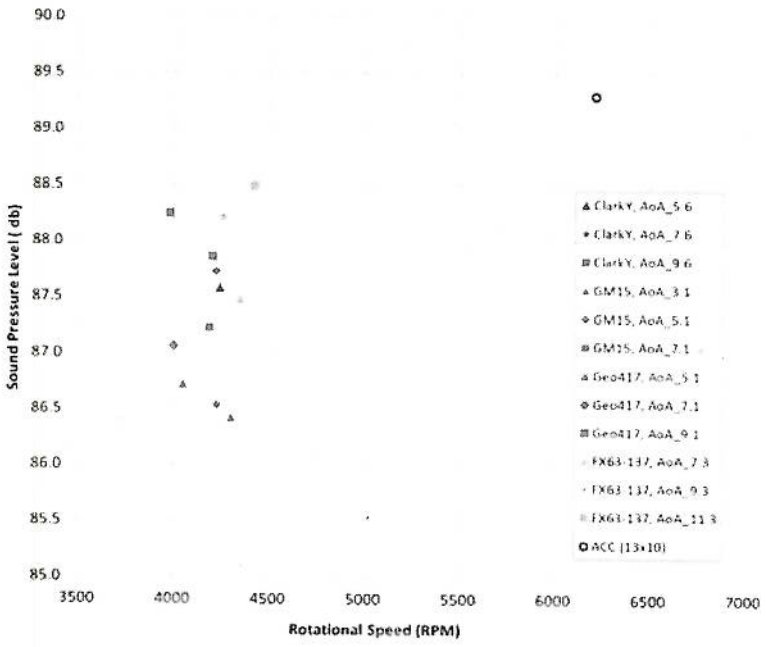

Figure 7. Sound pressure level as a function of the rotational speed required to achieve 2.5 lb$_f$ of thrust at a freestream velocity of 44 ft/s for the 12 airfoil propellers.

Figure 6 shows the aerodynamic efficiency as a function of the rotational speed required to achieve 2.5 lb$_f$ of thrust at a freestream velocity of 44 ft/s for the 12 airfoil propellers. Also included on this graph as a reference is the performance of the commercially available ACC 13x10 propeller. For each set of propellers, the lowest design/operating AoA has the highest aerodynamic efficiency and the highest AoA has the lowest aerodynamic efficiency. This trend would also extend to the overall efficiency as the propulsive efficiency is essentially the same for all 12 propellers because they all have the same diameter and same operating thrust at the design velocity of 44 ft/sec. Equation (16) shows that the aerodynamic efficiency is only a function of C_L/C_D and the inflow angle. Since the rotational speeds only vary by a few hundred RPM, the inflow angles for all 12 propellers are similar. The difference in aerodynamic efficiency can therefore be largely attributed to changes in C_L/C_D. C_L/C_D is the 3D lift to drag ratio which is a function of C_l/C_d (the airfoil lift to drag ratio), aspect ratio and the span efficiency factor. Span efficiency is largely a function of tip geometry. Since all these propellers have same flat tips, their span efficiencies are likely to be the very similar. Induced drag decreases as aspect ratio increases which increases C_L/C_D. The aspect ratio of the propellers does change due to the changes in chord length. However, if aspect ratio were the dominant affect one would expect to see an aerodynamic efficiency increase for the smaller chord length propellers designed at the higher AoAs. It appears as though the 2D airfoil performance (C_l/C_d)

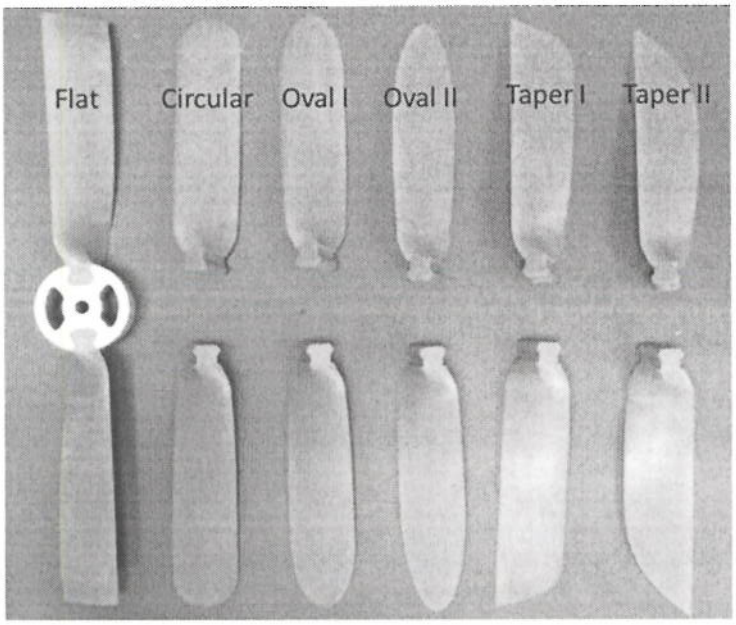

Figure 8. Constant chord propellers with different tip treatments.

based on the measured AoA dominates the aerodynamic efficiency trend. For each of the four sets of propellers, the one with the lowest designed AoA actually has the AoA closest to the AoA for maximum C_l/C_d and the highest aerodynamic efficiency. It is expected that higher aerodynamic efficiencies can be achieved from propellers designed with even lower AoAs. This AoA trend will be further explored in the section on hybrid propellers. The highest aerodynamic efficiency of the 12 propellers tested in this investigation is approximately one percentage point lower than the aerodynamic efficiency of the stock commercial ACC 13x10. The ACC 13x10 has a measured AoA = 5.6 deg which is about 2 deg lower than the AoA associated with the maximum C_l/C_d of the ClarkY airfoil that is used in this propeller. It's higher than expected aerodynamic efficiency is believed to be caused by the higher span efficiency associated with its pointed tip. The effect of tip geometry will be further explored in the following section.

Figure 7 shows the sound pressure level as a function of the rotational speed required to achieve 2.5 lb_f of thrust at a freestream velocity of 44 ft/s for the 12 airfoil propellers. For each set of propellers, the lowest design and operating AoA is the quietest (lowest sound pressure level) and the highest AoA is the loudest. This trend corresponds directly to the highest aerodynamic efficiency propeller being the quietest. The trend holds even though the high aerodynamic efficiency propellers have higher rotational speed which has been shown previously to

Table 2. Airfoil test series propeller characteristics and testing results. Results correspond to propeller generating 2.5 lb_f of thrust at a freestream velocity of 44 ft/s.

AirFoil	Design AoA *(deg)*	Chord *in*	Pitch *in*	Engine Speed *(RPM)*	Measured AoA *(deg)*	Aerodynamic Efficiency	Prop SPL *(dB)*
ClarkY	5.6	1.94	15.1	4241	8.3	0.75	87.6
ClarkY	7.6	1.61	16.4	4220	10.2	0.74	87.7
ClarkY	9.6	1.45	17.9	4202	12.1	0.72	87.9
GM15	3.1	1.86	13.4	4303	5.8	0.77	86.4
GM15	5.1	1.61	14.7	4226	7.6	0.76	86.5
GM15	7.1	1.43	16.1	4186	9.6	0.73	87.2
Geo417	5.1	1.78	14.7	4049	7.0	0.74	86.7
Geo417	7.1	1.51	16.1	4000	8.8	0.72	87.1
Geo417	9.1	1.31	17.5	3976	10.8	0.70	88.2
FX63-137	7.3	1.78	16.2	4346	10.4	0.74	87.5
FX63-137	9.3	1.51	17.6	4255	12.0	0.71	88.2
FX63-137	11.3	1.31	19.1	4417	14.6	0.70	88.5

Table 3. Tip treatment test series results corresponding to propeller generating 2.5 lb_f of thrust at a freestream velocity of 44 ft/s.

AirFoil	Tip	Engine Speed (RPM)	Measured AoA (deg)	Aerodynamic Efficiency	Prop SPL (dB)
ClarkY	Flat	4423	9.9	0.75	87.6
ClarkY	Round	4489	10.3	0.76	86.3
ClarkY	Oval 1	4641	10.7	0.77	86.2
ClarkY	Oval 2	4734	10.9	0.80	85.6
ClarkY	Taper 1	4641	10.7	0.75	87.2
ClarkY	Taper 2	4999	11.9	0.74	87.7

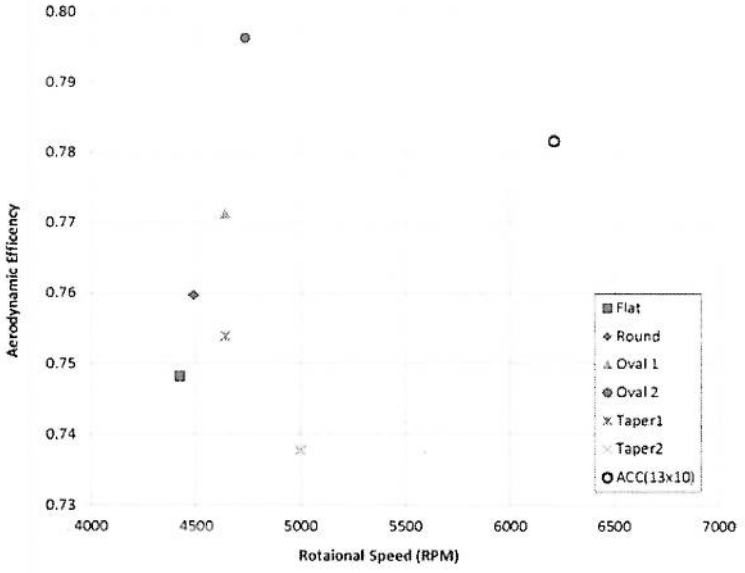

Figure 9. Aerodynamic efficiency as a function of the rotational speed required to achieve 2.5 lb_f of thrust at a freestream velocity of 44 ft/s for the 6 tip treatment propellers.

increase SPL. However, all of the flat tip propellers are significantly quieter than the stock ACC 13x10 propellers which rotates almost 2,000 RPM more to produce the same amount thrust. Lowering rotational speed is still a high priority for this investigation which has been demonstrated by the large chord propeller designs. However, this airfoil investigation suggests that induced drag generated at the tip of the propeller will lower aerodynamic efficiency and must also be considered. The tip treatment study in the next section explores the relationship between tip treatments and efficiency.

D. Tip Treatment Propellers

A series of propellers with special tip treatments were designed and fabricated based on a constant chord profile and are shown in shown in Figure 8. The large surface area of the constant chord propeller helps lower the RPM necessary to achieve the thrust requirement while the tip treatment decreases the induce drag and the strength of the vortex generated at the tip. These propellers all have the same ClarkY airfoil cross-section, 13.3 in overall diameter, chord length near the hub and pitch. The tip was not simply cut out of the constant chord flat tip propeller. Instead, the chord length was modified near the tip to establish the desired geometry while always maintaining the ClarkY airfoil cross-section. The results of this test series with each propeller generating 2.5 lb_f of thrust at 44 ft/s freestream velocity are listed in Table 3. The increased rotational speed required to achieve the operation thrust is the result of the reduced surface area created by the tip treatment. The Taper2 tip with the smallest surface area therefore requires the largest rotational speed. Unfortunately these are operating at a measured AoA much higher than required for the optimal C_l/C_d (AoA = 7.6 deg for the ClarkY airfoil) which significantly lowers the aerodynamic efficiency for all the propellers. However, since the AoA are all within 2 deg, relative comparisons can still be made.

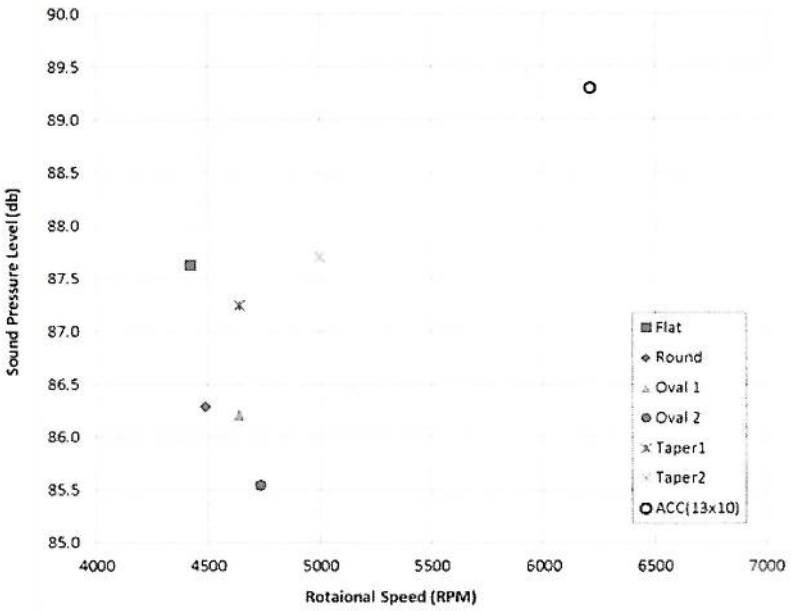

Figure 10. Sound Pressure level as a function of the rotational speed required to achieve 2.5 lb_f of thrust at a freestream velocity of 44 ft/s for the 6 tip treatment propellers.

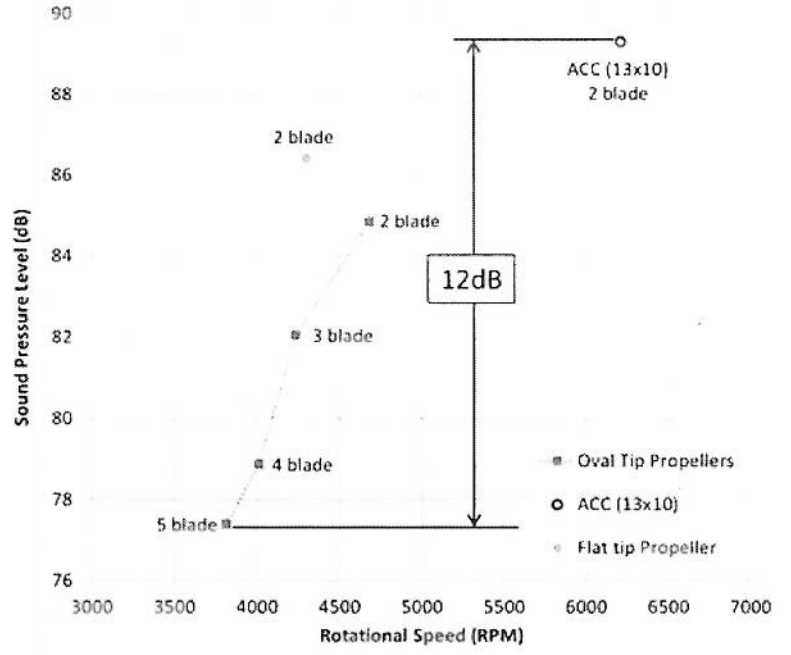

Figure 11. Sound Pressure Level as a function of the rotational speed required to achieve 2.5 lb_f of thrust at a freestream velocity of 44 ft/s for the hybrid GM15 airfoil oval tip propellers.

Figure 9 shows the aerodynamic efficiency as a function of the rotational speed required to achieve 2.5 lb_f of thrust at a freestream velocity of 44 ft/s for the 6 tip treatment propellers. The Oval2 tip treatment is the clear winner achieving an aerodynamic efficiency of 0.80, 2.5 percentage points higher than the Oval1 tipped propeller and 6 percentage points higher than the Taper2 tipped propeller. Since these propellers are all operating near the same AoA and have essentially the same aspect ratio, the increased aerodynamic efficiency must be attributed to an increase in span efficiency factor that in turn increases the 3D lift to drag ratio of the propeller. The Oval2 tip geometry was not designed with any particular lift distribution in mind. It is simple a narrower Oval contour than the Oval1 tip. A more sophisticated approach would be to design a tip contour that approximates an elliptical lift distribution. The plan is to investigate this possibility but the rotation of the propeller and pressure rise across it would make this design approach a significant challenge.

Figure 10 shows the sound pressure level as a function of the rotational speed required to achieve 2.5 lb_f of thrust at a freestream velocity of 44 ft/s for the 6 tip treatment propellers. The Oval2 propeller outperforms the others again demonstrating the importance of high aerodynamic efficiency. Figures 9 and 10 also include results of the baseline ACC13x10 propeller for reference. The Oval2 propeller has a modest ~1 percentage point increase in aerodynamic efficiency of the over the ACC13x10 propeller but a rather dramatic 4.5 dB decrease

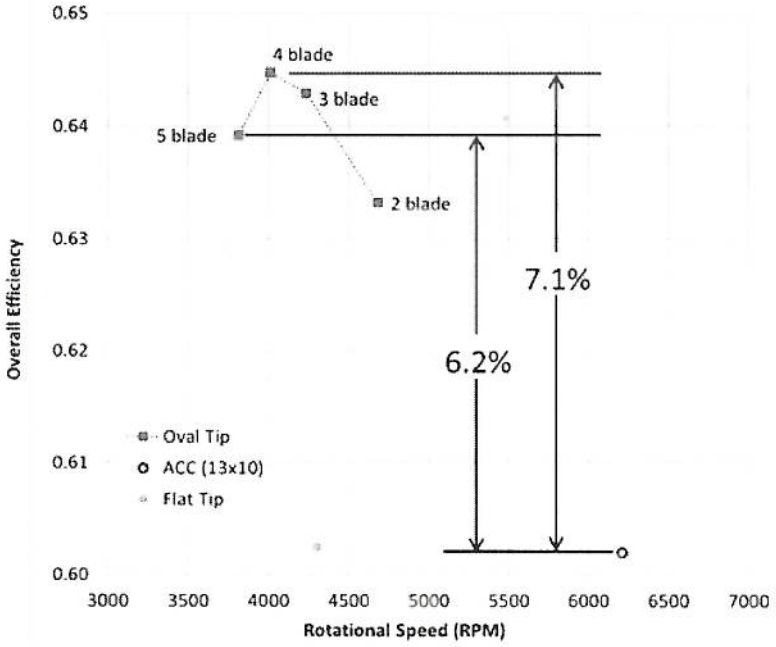

Figure 12. Overall efficiency as a function of the rotational speed required to achieve 2.5 lb_f of thrust at a freestream velocity of 44 ft/s for the hybrid GM15 airfoil oval tip propellers.

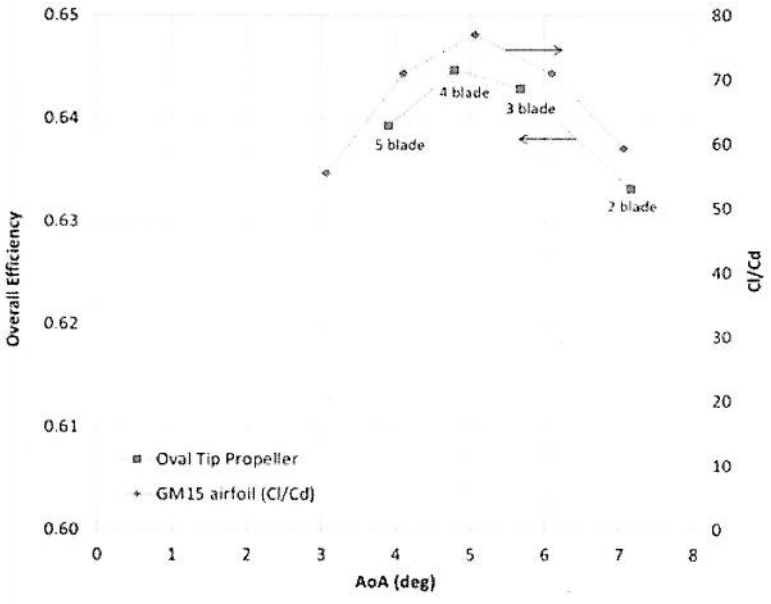

Figure 13. Overall efficiency as a function of the calculated angle of attack at the rotational speed required to achieve 2.5 lb_f of thrust at a freestream velocity of 44 ft/s for the hybrid GM15 airfoil oval tip propellers. Also shown on the secondary axis is the lift to drag ratio for the propeller airfoil cross-section (GM15).

in sound pressure level further reinforcing the importance of lowering the rotational speed.

E. Hybrid and Multi-bladed Propellers

A 13.3 in diameter propeller was designed with the GM15 airfoil and pitch of 13.4 in with an Oval2 tip geometry and tested with 2, 3 and 4 blades (note: the 3 and 4 bladed propellers have the same chord and beta angle distribution as the 2 bladed prop. The blades were not redesigned—only more blades added). This represents a combination of the best airfoil and the best tip treatment from the previous two test series. A 15 in diameter propeller with the GM15 airfoil and the Oval2 tip was also designed and tested. This prop had the same chord length as the 13.3 in diameter version but with a different beta distribution giving it a pitch of 11.7 in. Figures 11 and 12 show the sound pressure level and aerodynamic efficiency, respectively as a function of rotational speed required to achieve 2.5 lb_f of thrust at 44 ft/s freestream velocity for the hybrid propellers. Interpreting these results is difficult because so many parameters are change from propeller to propeller making it difficult to represent this on 2D graphs. Going from the 2 bladed flat tip to the 2 bladed oval tip propeller the aerodynamic efficiency increases by 4 percentage points and the SPL decreases by 1.6 dB. The oval tip lowers the vortex strength at the tip which is likely due to the lower induced drag created by the higher span efficiency factor which increases aerodynamic efficiency and lowers SPL. However, the lower surface area of the oval tip requires a higher rotational speed which will increase the tip vortex strength

lowering aerodynamic efficiency and increasing SPL. In addition, the higher rotational speed required by the oval tip propeller increases the measured AoA to 7.2 deg which is ~2 deg higher that the optimal for maximum C_l/C_d which will further decrease aerodynamic efficiency and increase SPL. The fact that aerodynamic efficiency increases and SPL decreases with addition of the oval tip indicates that tip geometry is the dominate factor over these small changes to rotational speed.

Adding blades to the oval propeller increases aerodynamic efficiency and lowers SPL. The aerodynamic efficiency increases but only by 1 percentage point for each additional blade while the SPL decreases by 2+ dB. It appears as though there are two competing circumstances. The rotational speed decreases due to the increase in surface area which will weaken the tip vortex and the efficiency increases because the AoA gets closer to the optimal. Both of these will work to lower the SPL. The measured 4.8 deg AoA is only slightly less than the optimal 5.1 deg AoA and it appears as though the aerodynamic efficiency has reached a peak and begun to decrease. This gives confidence in the measured AoA calculation which is noticeably different than the propeller design code QMIL/QPROP that predicts ~3deg AoA difference. These results have deviated significantly from the Sound Pressure Level vs Rotational Speed trend established by the ACC props but this is to be expected since the geometry (aspect ratio, chord lengths, etc.) are so different. The bottom line is that high aerodynamic efficiency correlates to low SPL. Not only does the 4 bladed oval tipped propeller decrease the SPL by over 10 dB it also increases the efficiency by almost 5 percentage points.

A fifth blade was added to the oval tip propeller configuration. This further lowered the rotational speed required to achieve 2.5 lb_f of thrust at 44 ft/s resulting in a 12 dB decrease in the sound pressure level from the stock ACC13x10 propeller as shown in Fig. 13. As expected the addition of a fifth blade decreased the overall efficiency. This is due to the lower AoA created by the lower rotational speed for the same pitched propeller which moves the propeller operating point away from its optimal C_l/C_d. Figure 13 shows the overall efficiency as a function of the calculated angle of attack at the rotational speed required to achieve 2.5 lb_f of thrust at a freestream velocity of 44 ft/s for the oval tip and tip vane propellers. Also shown on the secondary axis in this figure is the ratio of the lift to drag coefficients for the propeller airfoil cross-section (GM-15). This figure shows that the AoA for maximum overall efficiency of the oval tip propellers is in excellent agreement with the AoA for maximum C_l/C_d of the propeller airfoil cross-section. Since the propeller blades all have the same oval tip treatment they have the same span efficiency factor making the 2-D airfoil aerodynamics the dominate parameter effecting overall performance. This suggests that adding blades to the propeller configuration does not create significant interference issues with blades passing through each other's wakes. Adding ~1.5deg to the pitch of the oval tip blades and running it in the 5 bladed configuration should increase the operating AoA moving it closer to the optimal C_l/C_d increasing its overall efficiency and further decreasing SPL.

III Conclusions

A study was done to examine the influence of airfoil shape, tip geometry, Reynolds number and chord length on small propeller performance and noise. A set of four airfoils were selected based upon low Reynolds number performance and served as the cross-sections for custom designed propellers. These propellers also tested variations in design AoA. Airfoils selected based upon low Reynolds number performance resulted in increased overall efficiency and lower sound pressure levels. The GM15, with the highest maximum C_l/C_d for the tested airfoils, at an AoA of 3.1 performed the best for 2 bladed propellers. Another study tested six different tip treatments. The tip treatments were designed to improve the span efficiency factor and resulted in increased overall efficiency and lower sound pressure levels. The Oval2 performed the best for 2 bladed propellers. After these tests, a hybrid propeller consisting of the most efficient airfoil cross-section, the GM15, was coupled with the most efficient tip, the Oval2. This configuration was tested in the 2, 3, 4, and 5 bladed configuration. Increasing the number of blades from two to five resulted in lower rotational speeds required to achieve the required thrust and lower values of sound pressure levels. The general result with these tests was an increased overall efficiency and lower sound pressure level when compared to a stock, commercial propeller operating under the same conditions.

Acknowledgments

The authors would like to thank the United States Special Operations Command for their support of this research. Also, thanks go to the USAF Academy and Baylor University for providing the facilities and resources to accomplish the experimental testing

References

[1]"Froude's Propeller Theory". Aerodynamics for Students, Aerospace, Mechanical and Mechatronic Engineering, University of Sydney, 2005.

[2]Glauert Blade Element Theory, "Analysis of Propellers," Aerodynamics for Students, 1998-2012.

[3]Mattlingly, J.D., Heiser, W.H., and Pratt, D. T., "Aircraft Engine Design," Propeller Design Tools, 2nd ed., AIAA Education Series, Virginia, 2002, pp. 609-622.

[4]Wisniewski, C. F., Byerley, A. R., Heiser, W. H., Van Treuren, K. W., Liller, W. R., and Wisniewski, N., "Experimental Evaluation of Open Propeller Aerodynamic Performance and Aero-acoustic Behavior," AIAA 33rd Applied Aerodynamics Conference, Dallas, TX, June 22-26, 2015

[5]Kline, J. S., and McClintock, F. A., "Describing Uncertainties in Single-Sample Experiments," *ASME Journal of Mechanical Engineering*, January 1953, pp. 3-8.

[6] Selig, M., UIUC, Department of Aerospace Engineering, UIUC Airfoil Coordinates Database, http://m-selig.ae.illinois.edu/ads/coord_database.htmll, accessed on May 12, 2015.

[7]Drela, Mark, 2006, "QPROP Formulation," http://web.mit.edu/drela/Public/web/qprop/ accessed on April 29, 2015.

[8]Wisniewski, C. F., Byerley, A. R., Heiser, W. H., Van Treuren, K. W., and Liller, W. R., "Designing Small Propellers for Optimum Efficiency and Low Noise Footprint," AIAA 33rd Applied Aerodynamics Conference, Dallas, TX, June 22-26, 2015